Uncertainties in Tropical Pacific Ocean Simulations : The Seasonal and Interannual Sea Level Response to Three Analyses of the Surface Wind Field

Antonio J. BUSALACCHI[1], Michael J. McPHADEN[2], Joël PICAUT[3] and Scott SPRINGER[4]

[1] *Laboratory for Oceans, NASA / Goddard Space Flight Center Greenbelt, Maryland - U.S.A.*

[2] *NOAA / Pacific Marine Environmental Laboratory Seattle, Washington - U.S.A.*

[3] *Groupe SURTROPAC, ORSTOM Nouméa - New Caledonia.*

[4] *School of Oceanography, University of Washington Seattle, Washington - U.S.A.*

ABSTRACT

The purpose of this study is to characterize differences in the time/space structure present among conventional descriptions of the tropical Pacific surface wind field, and in turn, to quantify the impact of these differences on our ability to model the dominant wind-forced variability of the tropical Pacific Ocean on seasonal and interannual time scales. A linear, multiple vertical mode ocean model is used as a transfer function to determine the influence of three distinct surface wind stress products for the period 1979-1983. This five-year period was chosen for study because it encompasses three years of a fairly regular seasonal cycle leading up to the 1982-83 El Niño for which there are several coincident oceanic and surface wind data sets. The three different wind analyses used are the Florida State University subjective analysis, the University of Hawaii subjective analysis, and the Fleet Numerical Oceanography Center objective analysis. We examine first the three mean seasonal cycle solutions prior to El Niño which then serve as self-consistent bases for analyzing the significant anomalies about the mean in 1982-83.

The impact of uncertainties in the forcing functions is discussed relative to the dominant seasonal and interannual scales of variability for the wind-driven oceanic response. On seasonal time scales, critical differences in the wind stress products, of order 0.2-0.4 dynes cm^{-2}, were in wind regimes of surface convergence and significant gradients such as the ITCZ and SPCZ. These uncertainties in the wind fields were manifested in model sea level solutions as 6-12 cm discrepancies near the NECC Trough and east of New Guinea. On interannual time scales, the influence of greater sampling along the major ship tracks was evident. Away from the major shipping lanes rms differences in the wind stress anomalies (1979-1983) about the mean seasonal cycle (1979-1981) reached up to 0.5 dynes cm^{-2}. The combined effect of these differences in the wind products resulted in 8-20 cm rms differences in the model sea level simulations. The largest of these discrepancies tended to exist at the terminus of equatorial wave characteristics, e.g. in the east along the equator and in the west off the equator.

1. Introduction

Tropical ocean variability on time scales from months to years is considered to be principally deterministic (WCRP, 1985). In this regard the dynamic response of the tropical ocean is governed by the temporal and spatial structure of the surface wind stress. It follows that our ability to model accurately the upper tropical ocean circulation is intimately tied to our ability to describe accurately the surface wind field. Unfortunately, as a result of the logistical problems in monitoring the surface wind field over tropical oceans it is difficult to assess the accuracy of gridded fields of surface wind stress generated from sparse ship, buoy, island, or cloud motion observations or operational center analyses. Little is known even of the similarities or differences, on both seasonal and interannual time scales, among the various wind products presently available. The implications of possible and likely discrepancies and uncertainties in surface wind stress prescriptions for tropical ocean simulations is then also unknown.

The most straightforward way of assessing the dynamic, wind-driven response of the tropical ocean circulation is via vertically integrated variables, such as sea level, dynamic height, and heat content, which tend to average out nonlinear, nonadiabatic effects. Previous tropical Pacific model sea level studies have demonstrated that the quality of interannual hindcasts is higher along the equator and eastern boundary where the response is an integral function of the equatorial zonal wind stress to the west (Busalacchi and Cane, 1985). The quality of sea level hindcasts is degraded away from the equator where the solution is determined, in part, by a derivative of the forcing, i.e., the wind stress curl. Random errors present in wind stress data would tend to have a greater influence off the equator where they would be differentiated as opposed to on the equator where their effect would be integrated.

Recently, a series of numerical experiments have been performed in order to assess the impact of wind stress uncertainties on the dynamic response of wind-driven tropical Pacific Ocean simulations. McPhaden et al. (1988a) examined simulations of the mean seasonal cycle using a multiple vertical mode linear model forced with three different surface wind stress products averaged over the period 1979-1981. Simulated mean seasonal cycles in dynamic height and sea level were then compared with observed variations based on expendable bathythermograph (XBT) and island tide gauge data averaged over the same 1979-1981 period. Landsteiner et al. (1989) examined the Sverdrup responses to the three-year mean (1979-1981) wind stresses and compared those responses to XBT-derived pressures and transports for the same period. Busalacchi et al. (1989) extended these studies to consider the interannual variability for the five years 1979-1983 including the anomalies associated with the 1982-83 El Niño. This allowed the similarities and discrepancies between the three wind products on seasonal time scales to be quantified and intercompared with those on interannual time scales. The impact of the differences in the wind field was assessed by a similar treatment of the model sea level solutions. Related studies were also performed in which the model solutions were used to address array design and sampling questions pertaining to the XBT (McPhaden et al., 1988b) and sea level (Springer et al., 1989) observations. The purpose of the present note is to summarize succinctly the differences in the time/space structure present among conventional descriptions of the tropical Pacific surface wind field, and in turn, to quantify the impact of these discrepancies on our ability to model the dominant wind-forced variability of the tropical Pacific Ocean on seasonal and interannual time scales.

2. Wind Stress Products and Ocean Model

The period of interest, 1979-1983, was chosen because it provided an interesting contrast between a fairly regular mean seasonal cycle for 1979-1981 and the extreme El

Niño event that followed in 1982-83. More importantly, it was also a time for which there are three different wind stress products available, each resulting from a consistent analysis scheme over the full five years. Two of these data sets are derived from subjective analyses, and the third is derived from an operational objective analysis. One of the subjective analyses is the Florida State University (FSU) analysis of ship-board observations provided by J. J. O'Brien. The analysis procedure of transforming individual ship wind observations into monthly mean wind stress fields on a 2° x 2° grid is described by Goldenberg and O'Brien (1981). The second subjective analysis is a combination of satellite-observed, low-level cloud motion vectors, ship wind observations, island wind observations, and buoy wind observations performed by J. Sadler at the University of Hawaii. The production of monthly mean surface wind and wind stress data sets on a 2.5° x 2.5° grid is described by Sadler and Kilonsky (1985) and Sadler et al. (1987). The third data set is an objectively analyzed operational product from the Global Band Analyses of the U. S. Navy's Fleet Numerical Oceanography Center (FNOC). An objective analysis based on Cressman (1959) is used on all reports (ship, island, buoy, etc.) in an operational data base for 6-hour intervals on a 2.5° x 2.5° grid. Six-hourly stresses are computed and averaged to form monthly means. A constant drag coefficient of 1.5×10^{-3} is used to convert from wind to wind stress for each of the three wind data sets.

A linear, numerical treatment of the shallow water wave equations is used as a transfer function to analyze the wind-driven dynamic response of a model tropical Pacific Ocean to different representations of the surface wind stress. The model basin extends from 20°N to 20°S and 126°E to 70°W. For the purposes here, sea level is the variable of interest. In response to the monthly mean forcing from January 1979 to December 1983 model height field solutions are generated for the first four baroclinic modes. A final sea level solution is found by summing the individual contributions to sea level from each of the four vertical modes. We consider both the mean seasonal cycle of sea level during the pre-El Niño period 1979-1981 and the anomalies for 1979-1983 about the 1979-1981 mean seasonal cycle.

3. Results

In this note we will only focus on the zonal wind stress since it is the dominant component of the trade winds and the most important for driving the tropical ocean circulation. Root mean square (RMS) differences between all three wind stress products for both the seasonal cycle and interannual anomalies are used as a measure of the discrepancies and uncertainties among the three data sets. Similarly, rms differences between the three model sea level solutions are used to depict how the differences in the total wind stress forcing become manifest in the forced integrated response of sea level. Busalacchi et al. (1989) provide a more in depth treatment of the signal and uncertainty in the annual mean, seasonal variability, and interannual variability of the zonal wind stress, meridional wind stress, wind stress curl, and resultant model sea level response.

On seasonal time scales, as defined by the mean seasonal cycle for 1979-1981, the largest fluctuations for the zonal wind stress (standard deviations of 0.4-0.7 dynes cm^{-2}) are similar in all three wind products and are associated with the broad-band seasonal excursions of the Intertropical Convergence Zone (ITCZ) in the Northern Hemisphere and the monsoon circulation of both hemispheres in the far western portion of the basin. With this seasonal signal as background, the largest rms differences in the seasonal zonal wind stress, as shown in Figure 1, are of order 0.2-0.4 dynes cm^{-2} along 8°-10°N and in the Southern Hemisphere where there are few wind observations. The maximum rms differences usually coincide with the largest seasonal fluctuations, i.e., the error is largest where the signal is largest. Of the three rms product combinations, the FSU and Sadler zonal wind stress appear to be the most similar to each other and conversely the largest

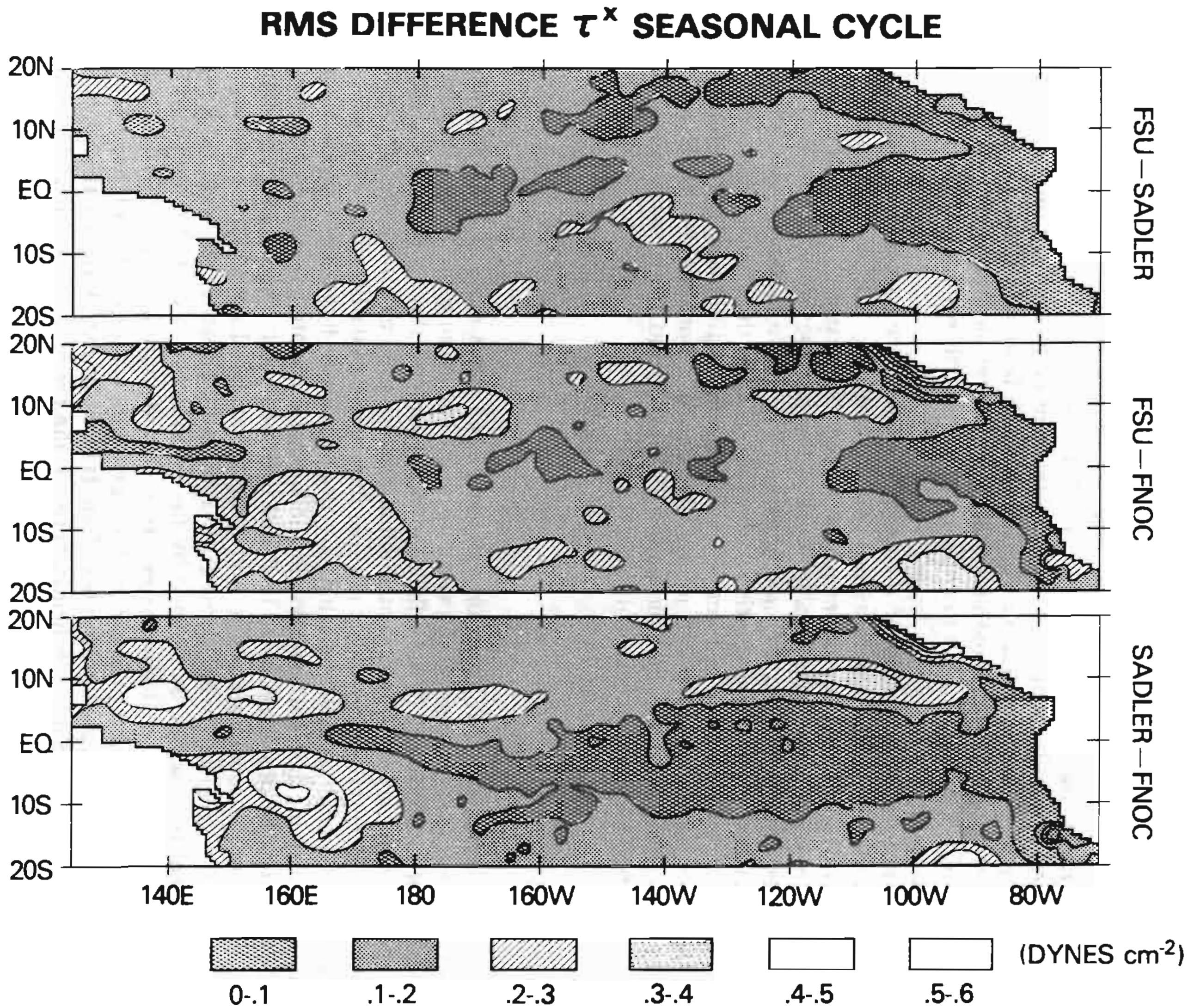

Figure 1. Root mean square difference between the seasonal cycles (1979-1981) of the zonal wind stress for a) FSU - Sadler b) FSU - FNOC c) Sadler - FNOC

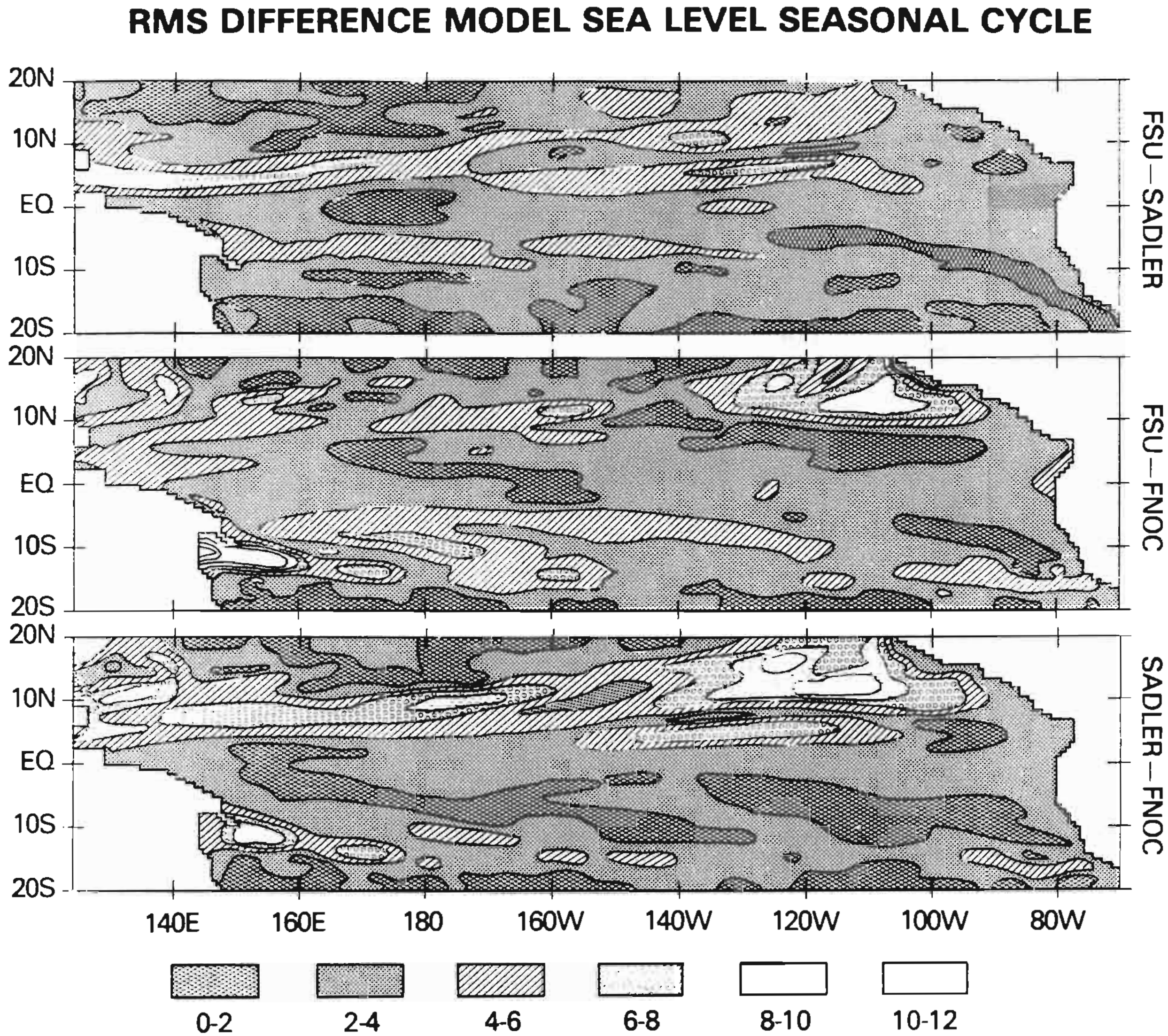

Figure 2. Root mean square difference between the seasonal cycles (1979-1981) of the wind-driven model sea level for a) FSU - Sadler b) FSU - FNOC c) Sadler - FNOC

rms differences are with the FNOC data. In general, the rms differences are less than the standard deviation of the seasonal cycle when viewed on the basin scale. If the discrepancies that the rms differences represent are taken to be a measure of the uncertainty or noise within the forcing data and the seasonal standard deviations as signal, then a crude signal/noise measure of approximately 1.5 is obtained for the seasonal zonal wind stress. A similar measure is also found for the seasonal meridional wind stress.

Whereas the basin-scale structure of the seasonal variability for the three zonal wind stress products was similar, the sea level responses to the total wind stress forcing are dissimilar. The only aspect of the seasonal response common to all three solutions is a region of maximum variability of 6-9 cm in the northeast corner of the basin. The rms differences between the three seasonal sea level solutions are shown in Figure 2. The largest differences, of order 6-9 cm, are in the vicinity of the North Equatorial Countercurrent (NECC) Trough beneath the ITCZ and are of similar amplitude to the maximum of the seasonal sea level response. The location of these differences signifies major inconsistencies in the seasonal variability and structure for the NECC and North Equatorial Current across the entire basin in the three solutions. The most significant of these differences is found to occur between the Sadler and FNOC forced solutions. Other notable differences, from 4-12 cm, are found beneath the South Pacific Convergence Zone (SPCZ) in the southwestern tropical Pacific. As a result of equatorial wave radiation away from regions of significant forcing, uncertainties in the wind stress can propagate to points far beyond the region of forcing. Thus, the signal to noise ratio of 1.5 that characterized the zonal and meridional wind stress components does not hold for the integrated response of the model sea level. The rms differences in sea level across the basin are nearly equivalent to the mean seasonal sea level signal implying a signal to noise ratio of 1.

The interannual variability is addressed by considering the anomalies for 1979-1983 about the mean seasonal cycle for the pre-El Niño years of 1979-1981. In terms of the zonal wind stress, the largest anomalous variations are in the central equatorial Pacific between 140°W and 160°W of 0.4-0.5 dynes cm^{-2} for both the FSU and Sadler products. The maximum anomalies for FNOC are smaller and further to the east. Inspection of individual monthly anomaly maps indicates this region of maximum interannual variability is the result of equatorial westerly anomalies during the onset of the 1982-83 El Niño. The basin-wide mean for this interannual signal is approximately 0.25 dynes cm^{-2} for all three products. The largest rms differences in the anomalies of the zonal wind stress, between 0.25-0.5 dynes cm^{-2}, are also located in the central equatorial Pacific (Fig. 3). A second area of large rms differences is in the Northern Hemisphere between 160°E and 170°W. Bordering these regions we are able to see the influence of denser sampling along the major shipping lanes. From Fiji to the Philippines/Japan and Fiji to Hawaii/North America the rms differences are often between 0.1-0.2 dynes cm^{-2}. For these specific regions of enhanced observations the signal/noise is greater than 1. Away from these ship tracks the rms differences in the wind stress anomalies may reach up to 0.5 dynes cm^{-2} and hence the signal to noise is considerably less than 1.

In response to the five years of anomalous zonal and meridional wind stress forcing, the largest interannual sea level variability in the FSU and Sadler solutions is in the southwestern Pacific of 12-15 cm. Another region of large variability is a symmetric equatorial response found in the east of 9-12 cm. As in the wind stress forcing the most significant sea level anomalies occur during the 1982-83 El Niño. The FSU and Sadler sea level solutions are clearly the most similar (Fig. 4). Root mean square differences range between 4 and 12 cm and imply a basin-wide signal to noise ratio greater than 1. The rms differences involving the FNOC forced sea level solutions are considerably larger and exhibit broad regions of sea level discrepancies greater than 12 cm. The signal to noise ratio for the two product combination involving FNOC are

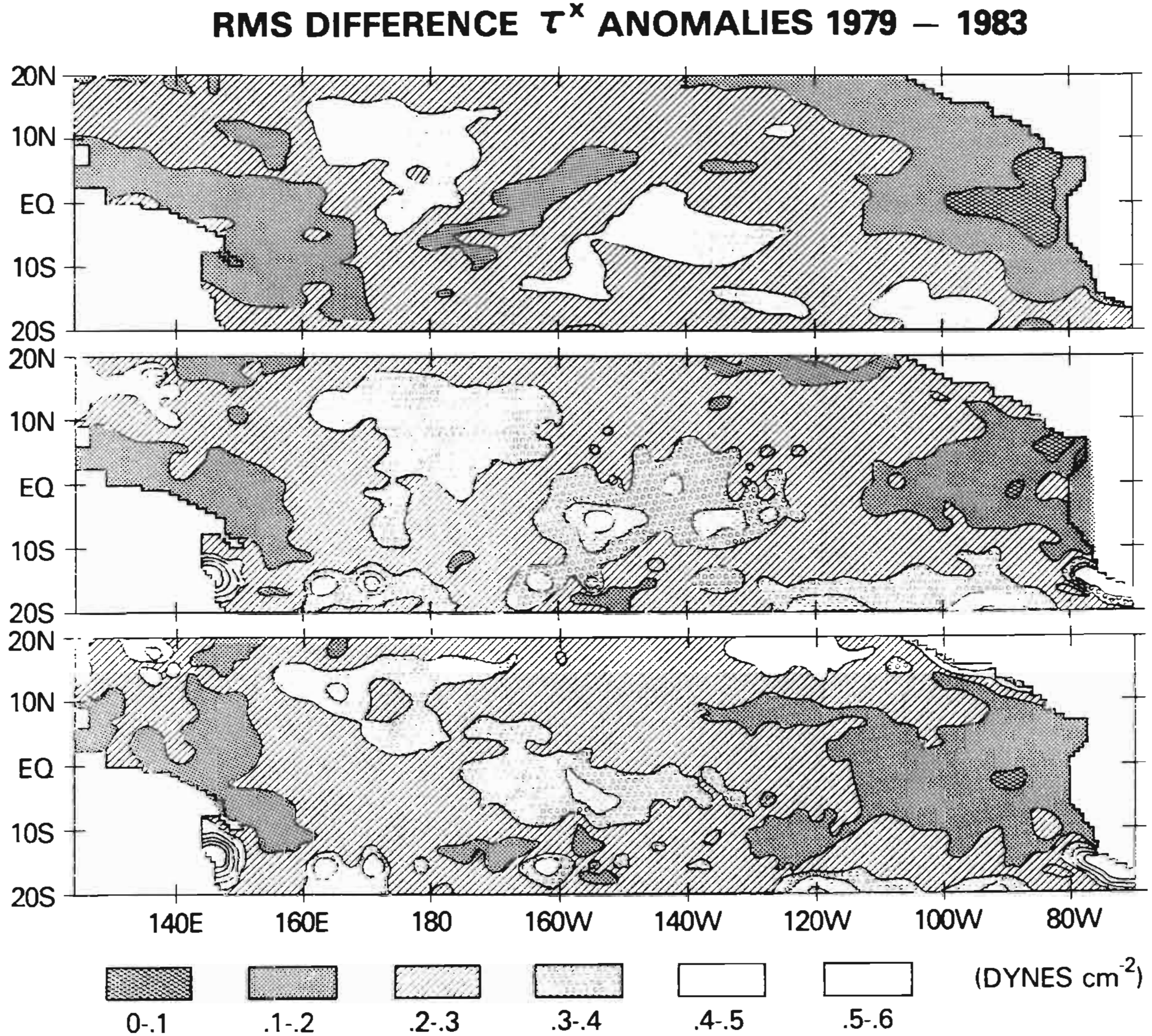

Figure 3. Root mean square difference between the anomalies (1979-1983) about the mean seasonal cycle (1979-1981) of the zonal wind stress for
a) FSU - Sadler b) FSU - FNOC c) Sadler - FNOC

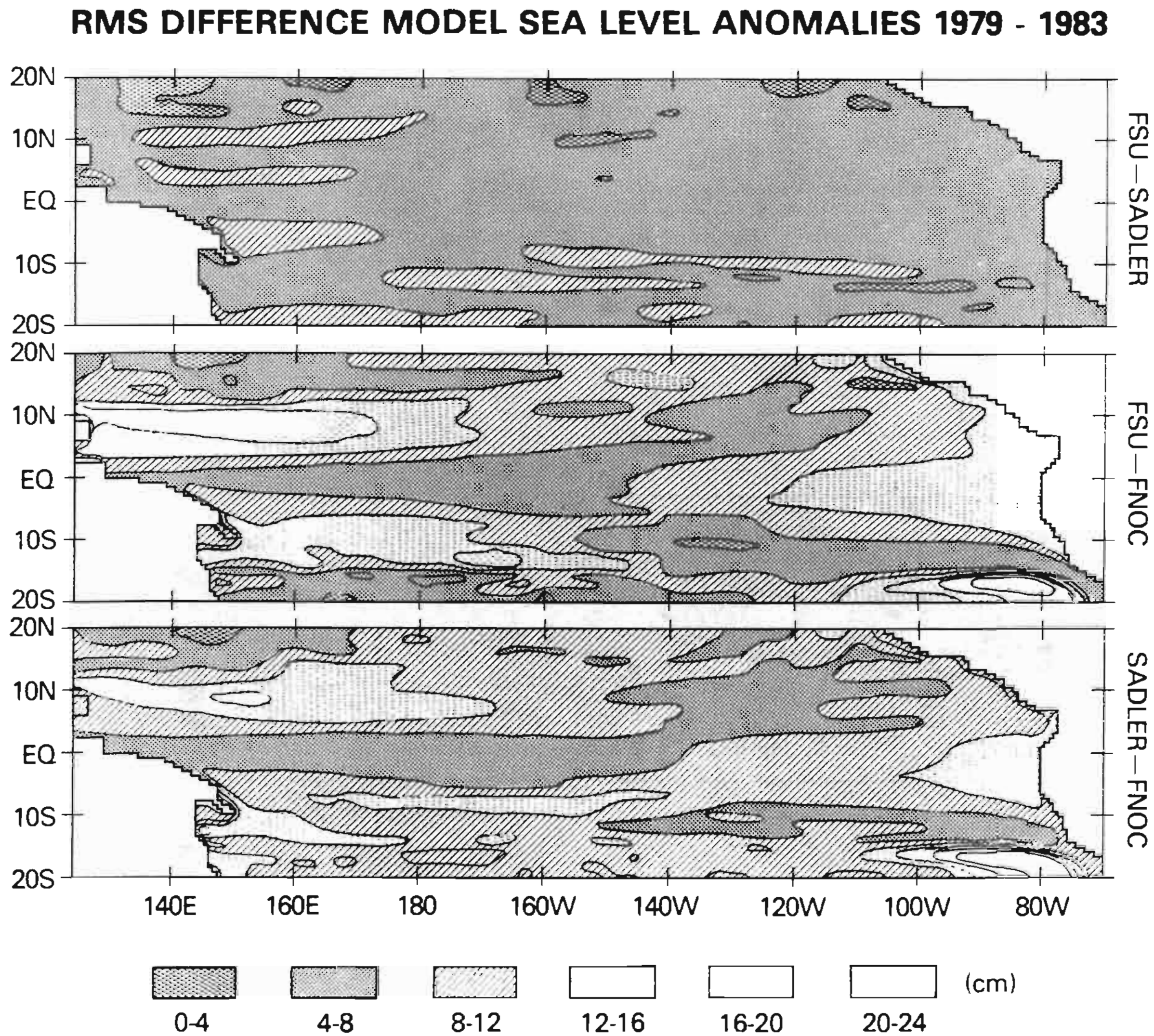

Figure 4. Root mean square difference between the anomalies (1979-1983) about the mean seasonal cycle (1979-1981) of the wind-driven model sea level for
a) FSU - Sadler b) FSU - FNOC c) Sadler - FNOC

significantly less than 1. Characteristic of all three rms difference pairs is an increase in the direction of equatorial wave propagation, i.e., from west to east along the equator and from east to west off the equator.

4. Discussion and Conclusions

The principal objective of this activity was to acquire, analyze, and intercompare "conventional" wind stress products for the tropical Pacific Ocean on seasonal and interannual time scales. Subsequently, these data were used to drive a linear, multi-mode numerical ocean model wherein the model served as a transfer function for the integrated response to the various wind forcings. On seasonal time scales, some of the greatest differences among the FSU, Sadler, and FNOC wind stress products, of order 0.2-0.4 dynes cm^{-2}, were in wind regimes of surface convergence and significant gradients such as the ITCZ and SPCZ. These uncertainties in the wind fields were manifested in model sea level solutions as 6-12 cm discrepancies near the NECC Trough and east of New Guinea. On interannual time scales, the influence of greater sampling along the major ship tracks was evident. Away from the major shipping lanes rms differences in the anomalies (1979-1983) about the mean seasonal cycle (1979-1981) reached up to 0.5 dynes cm^{-2}. The combined effect of these differences in the wind products resulted in 8-20 cm rms differences in the model sea level simulations. The largest of these discrepancies tended to exist at the terminus of equatorial wave characteristics, e.g. in the east along the equator and in the west off the equator.

The results presented here indicate that of the three wind stress products, the FSU and Sadler data were the most consistent on both seasonal and interannual time scales. The same held true for the sea level solutions forced by these data sets. The largest discrepancies were found to occur with the FNOC zonal wind stress and FNOC driven sea level solution. The signal/noise ratios, or more correctly the signal/uncertainty ratios, that were used to characterize these wind data and wind-forced solutions tend to support previous intercomparisons of the model sea level with XBT-derived dynamic heights and tide gauge observations. McPhaden et al. (1988a) found coherence estimates of 0.5-0.7 between the three model simulations and the observations for the 1 cycle per year harmonic, which dominates the seasonal cycle over most of the tropical Pacific. However, no wind stress product was capable of being judged to be clearly superior to the others based on the comparisons of the model sea level and dynamic height solutions with the in-situ observations. Although the signal to noise ratio for the seasonal cycle of the zonal wind stress was greater than one, this measure yields little information regarding how well gradients in the wind stress are being described, e.g. $\partial\tau^x/\partial y$. When the seasonal variability is considered in terms of the wind stress curl, which is the most appropriate representation of the wind stress when considering the off-equatorial oceanic response, the signal to noise is reduced to one. This is consistent with the signal to noise estimated for the seasonal model sea level response.

For the interannual variability, Busalacchi et al. (1989) correlated the time series of sea level anomalies from the model solutions with those observed at 36 island and coastal stations. The correlations were based on typically four to five years of data spanning 1979-1983. The overall quality of the FSU forced and Sadler forced sea level solutions was virtually indistinguishable. Cross correlations between the FSU forced solutions with the observed sea level ranged between -0.01 to 0.93 with an ensemble mean correlation coefficient of 0.58. Cross correlations between the Sadler forced solutions with the observed sea level ranged between -0.45 to 0.98 and also had a mean correlation coefficient of 0.58. The skill of the hindcast driven by FNOC winds was significantly less. Correlation coefficients ranged between -0.74 to 0.74 with an ensemble mean correlation of only 0.17. Consistent with these intercomparisons are the signal/noise ratios for the anomalous sea level solutions that are greater than 1 between FSU and Sadler but less than 1 when involving FNOC.

Only the FSU, Sadler, and FNOC wind stress data sets were considered to be permissible for our analyses of the seasonal and interannual variability as these were the only products available for which there was a consistent analysis scheme in place for the entire five year period. Periodic improvements and changes to the analysis schemes at other operational centers such as ECMWF and NMC precluded the use of these products. Nonetheless, an internally consistent analysis scheme is essential to any research investigation of interannual variability. The importance of the El Niño phenomenon brings this issue to the forefront. By restricting their focus to only the 1982-1983 El Niño, Harrison et al. (1989) were recently able to consider the response of an ocean general circulation model to the three wind sets considered here as well as the operational wind fields from NMC and ECMWF. Comparison of dynamic heights from the primitive equation model solutions with those derived from ship-of-opportunity XBT data also indicated better hindcast skill for the solutions forced by the subjective analyses than the operational center analyses. The problems encountered in these types of modelling studies clearly demonstrate the need, sometime during the TOGA decade, for a reanalysis of atmospheric model based data, such that a multiyear record of surface winds is produced with an internally consistent analysis. The subsequent use and scrutiny of these winds in ocean simulation studies will prove very useful in evaluating the reanalyzed atmospheric data.

References

Busalacchi, A. J., and M. A. Cane, Hindcasts of sea level variations during the 1982-83 El Niño, *J. Phys. Oceanogr.*, *15*, 213-221, 1985.

Busalacchi, A. J., M. J. McPhaden, J. Picaut, and S. Springer, Sensitivity of wind-driven tropical Pacific ocean simulations on seasonal and interannual time scales, to appear in Coupled Ocean-Atmosphere Models: Proceedings of the 21st International Liege Colloquium on Ocean Hydrodynamics, J.C.J. Nihoul, Ed., Elsevier, 1989.

Cressman, G. P., An operational objective analysis system, *Mon. Weather Rev.*, *87*, 367-374, 1959.

Goldenberg, S. B., and J. J. O'Brien, Time and space variability of tropical Pacific wind stress, *Mon. Wea. Rev.*, *109*, 1190-1207, 1981.

Harrison, D. E., W. S. Kessler, and B. S. Giese, Ocean circulation model hindcasts of the 1982-83 El Niño: Thermal variability along the ship-of-opportunity tracks, *J. Phys. Oceanogr.*, *19*, 397-418, 1989.

Landsteiner, M. C., M. J. McPhaden, and J. Picaut, On the sensitivity of Sverdrup transport estimates to the specification of wind stress forcing in the tropical Pacific, J. Geophys. Res., (in press), 1989.

McPhaden, M. J., A. J. Busalacchi, J. Picaut, and G. Raymond, A model study of potential sampling errors due to data scatter around expendable bathythermograph transects in the tropical Pacific, *J. Geophys. Res.*, *93*, 8119-8130, 1988a.

McPhaden, M. J., A. J. Busalacchi, and J. Picaut, Observations and wind-forced model simulations of the mean seasonal cycle in tropical Pacific Sea Surface Topography, *J. Geophys. Res.*, *93*, 8131-8146, 1988b.

Sadler, J. C., and B. J. Kilonsky, Deriving surface winds from satellite observations of low-level cloud motions, *J. Clim. Appl. Meteorol.*, *24*, 758-769, 1985.

Sadler, J. C., M. A. Lander, A. M. Hori, and L. K. Oda, Tropical marine climatic atlas, II, Pacific Ocean, *Tech. Rep. UHMET 87-02*, Dep. of Meteorol., Univ. of Hawaii, Honolulu, 1987.

Springer, S., M. McPhaden, and A. J. Busalacchi, Oceanic heat content variability during the 1982-83 El Niño, (manuscript in preparation), 1989.

World Climate Research Program, Scientific Plan for the Tropical Ocean and Global Atmosphere Programme, 146pp., WCRP Publications Series No. 3, 1985.

WESTERN PACIFIC INTERNATIONAL MEETING AND WORKSHOP ON TOGA COARE

Nouméa, New Caledonia
May 24-30, 1989

PROCEEDINGS

edited by

Joël Picaut *
Roger Lukas **
Thierry Delcroix *

* ORSTOM, Nouméa, New Caledonia
** JIMAR, University of Hawaii, U.S.A.

INSTITUT FRANÇAIS DE RECHERCHE SCIENTIFIQUE
POUR LE DÉVELOPPEMENT EN COOPÉRATION

ORSTOM

Centre de Nouméa

TABLE OF CONTENTS

ABSTRACT i

RESUME iii

ACKNOWLEDGMENTS vi

INTRODUCTION

1. Motivation 1
2. Structure 2

LIST OF PARTICIPANTS 5

AGENDA 7

WORKSHOP REPORT

1. Introduction 19
2. Working group discussions, recommendations, and plans 20
a. Air-Sea Fluxes and Boundary Layer Processes 20
b. Regional Scale Atmospheric Circulation and Waves 24
c. Regional Scale Oceanic Circulation and Waves 30
3. Related programs 35
a. NASA Ocean Processes and Satellite Missions 35
b. Tropical Rainfall Measuring Mission 37
c. Typhoon Motion Program 39
d. World Ocean Circulation Experiment 39
4. Presentations on related technology 40
5. National reports 40
6. Meeting of the International Ad Hoc Committee on TOGA COARE 40

APPENDIX: WORKSHOP RELATED PAPERS

Robert A. Weller and David S. Hosom: Improved Meteorological Measurements from Buoys and Ships for the World Ocean Circulation Experiment 45
Peter H. Hildebrand: Flux Measurement using Aircraft and Radars 57
Walter F. Dabberdt, Hale Cole, K. Gage, W. Ecklund and W.L. Smith: Determination of Boundary-Layer Fluxes with an Integrated Sounding System 81

MEETING COLLECTED PAPERS

WATER MASSES, SEA SURFACE TOPOGRAPHY, AND CIRCULATION

Klaus Wyrtki: Some Thoughts about the West Pacific Warm Pool 99
Jean René Donguy, Gary Meyers, and Eric Lindstrom: Comparison of the Results of two West Pacific Oceanographic Expeditions FOC (1971) and WEPOCS (1985-86) 111
Dunxin Hu, and Maochang Cui: The Western Boundary Current in the Far Western Pacific Ocean 123
Peter Hacker, Eric Firing, Roger Lukas, Philipp L. Richardson, and Curtis A. Collins: Observations of the Low-latitude Western Boundary Circulation in the Pacific during WEPOCS III 135
Stephen P. Murray, John Kindle, Dharma Arief, and Harley Hurlburt: Comparison of Observations and Numerical Model Results in the Indonesian Throughflow Region 145
Christian Henin: Thermohaline Structure Variability along 165°E in the Western Tropical Pacific Ocean (January 1984 - January 1989) 155
David J. Webb, and Brian A. King: Preliminary Results from Charles Darwin Cruise 34A in the Western Equatorial Pacific 165
Warren B. White, Nicholas Graham, and Chang-Kou Tai: Reflection of Annual Rossby Waves at The Maritime Western Boundary of the Tropical Pacific 173
William S. Kessler: Observations of Long Rossby Waves in the Northern Tropical Pacific 185
Eric Firing, and Jiang Songnian: Variable Currents in the Western Pacific Measured During the US/PRC Bilateral Air-Sea Interaction Program and WEPOCS 205
John S. Godfrey, and A. Weaver: Why are there Such Strong Steric Height Gradients off Western Australia ? 215
John M. Toole, R.C. Millard, Z. Wang, and S. Pu: Observations of the Pacific North Equatorial Current Bifurcation at the Philippine Coast 223

EL NINO/SOUTHERN OSCILLATION 1986-87

Gary Meyers, Rick Bailey, Eric Lindstrom, and Helen Phillips: Air/Sea Interaction in the Western Tropical Pacific Ocean during 1982/83 and 1986/87 229
Laury Miller, and Robert Cheney: GEOSAT Observations of Sea Level in the Tropical Pacific and Indian Oceans during the 1986-87 El Nino Event 247
Thierry Delcroix, Gérard Eldin, and Joël Picaut: GEOSAT Sea Level Anomalies in the Western Equatorial Pacific during the 1986-87 El Nino, Elucidated as Equatorial Kelvin and Rossby Waves 259
Gérard Eldin, and Thierry Delcroix: Vertical Thermal Structure Variability along 165°E during the 1986-87 ENSO Event 269
Michael J. McPhaden: On the Relationship between Winds and Upper Ocean Temperature Variability in the Western Equatorial Pacific 283

John S. Godfrey, K. Ridgway, Gary Meyers, and Rick Bailey: Sea Level and Thermal Response to the 1986-87 ENSO Event in the Far Western Pacific 291
Joël Picaut, Bruno Camusat, Thierry Delcroix, Michael J. McPhaden, and Antonio J. Busalacchi: Surface Equatorial Flow Anomalies in the Pacific Ocean during the 1986-87 ENSO using GEOSAT Altimeter Data 301

THEORETICAL AND MODELING STUDIES OF ENSO AND RELATED PROCESSES

Julian P. McCreary, Jr.: An Overview of Coupled Ocean-Atmosphere Models of El Nino and the Southern Oscillation 313
Kensuke Takeuchi: On Warm Rossby Waves and their Relations to ENSO Events 329
Yves du Penhoat, and Mark A. Cane: Effect of Low Latitude Western Boundary Gaps on the Reflection of Equatorial Motions 335
Harley Hurlburt, John Kindle, E. Joseph Metzger, and Alan Wallcraft: Results from a Global Ocean Model in the Western Tropical Pacific 343
John C. Kindle, Harley E. Hurlburt, and E. Joseph Metzger: On the Seasonal and Interannual Variability of the Pacific to Indian Ocean Throughflow 355
Antonio J. Busalacchi, Michael J. McPhaden, Joël Picaut, and Scott Springer: Uncertainties in Tropical Pacific Ocean Simulations: The Seasonal and Interannual Sea Level Response to Three Analyses of the Surface Wind Field 367
Stephen E. Zebiak: Intraseasonal Variability - A Critical Component of ENSO ? 379
Akimasa Sumi: Behavior of Convective Activity over the "Jovian-type" Aqua-Planet Experiments 389
Ka-Ming Lau: Dynamics of Multi-Scale Interactions Relevant to ENSO 397
Pecheng C. Chu and Roland W. Garwood, Jr.: Hydrological Effects on the Air-Ocean Coupled System 407
Sam F. Iacobellis, and Richard C.J. Somerville: A one Dimensional Coupled Air-Sea Model for Diagnostic Studies during TOGA-COARE 419
Allan J. Clarke: On the Reflection and Transmission of Low Frequency Energy at the Irregular Western Pacific Ocean Boundary - a Preliminary Report 423
Roland W. Garwood, Jr., Pecheng C. Chu, Peter Muller, and Niklas Schneider: Equatorial Entrainment Zone : the Diurnal Cycle 435
Peter R. Gent: A New Ocean GCM for Tropical Ocean and ENSO Studies 445
Wasito Hadi, and Nuraini: The Steady State Response of Indonesian Sea to a Steady Wind Field 451
Pedro Ripa: Instability Conditions and Energetics in the Equatorial Pacific 457
Lewis M. Rothstein: Mixed Layer Modelling in the Western Equatorial Pacific Ocean 465
Neville R. Smith: An Oceanic Subsurface Thermal Analysis Scheme with Objective Quality Control 475
Duane E. Stevens, Qi Hu, Graeme Stephens, and David Randall: The hydrological Cycle of the Intraseasonal Oscillation 485
Peter J. Webster, Hai-Ru Chang, and Chidong Zhang: Transmission Characteristics of the Dynamic Response to Episodic Forcing in the Warm Pool Regions of the Tropical Oceans 493

MOMENTUM, HEAT, AND MOISTURE FLUXES BETWEEN ATMOSPHERE AND OCEAN

W. Timothy Liu: An Overview of Bulk Parametrization and Remote Sensing of Latent Heat Flux in the Tropical Ocean 513
E. Frank Bradley, Peter A. Coppin, and **John S. Godfrey**: Measurements of Heat and Moisture Fluxes from the Western Tropical Pacific Ocean 523
Richard W. Reynolds, and **Ants Leetmaa**: Evaluation of NMC's Operational Surface Fluxes in the Tropical Pacific 535
Stanley P. Hayes, Michael J. McPhaden, John M. Wallace, and **Joël Picaut**: The Influence of Sea-Surface Temperature on Surface Wind in the Equatorial Pacific Ocean 543
T.D. Keenan, and **Richard E. Carbone**: A Preliminary Morphology of Precipitation Systems In Tropical Northern Australia 549
Phillip A. Arkin: Estimation of Large-Scale Oceanic Rainfall for TOGA 561
Catherine Gautier, and **Robert Frouin**: Surface Radiation Processes in the Tropical Pacific 571
Thierry Delcroix, and **Christian Henin**: Mechanisms of Subsurface Thermal Structure and Sea Surface Thermo-Haline Variabilities in the South Western Tropical Pacific during 1979-85 - A Preliminary Report 581
Greg. J. Holland, T.D. Keenan, and **M.J. Manton**: Observations from the Maritime Continent : Darwin, Australia 591
Roger Lukas: Observations of Air-Sea Interactions in the Western Pacific Warm Pool during WEPOCS 599
M. Nunez, and **K. Michael**: Satellite Derivation of Ocean-Atmosphere Heat Fluxes in a Tropical Environment 611

EMPIRICAL STUDIES OF ENSO AND SHORT-TERM CLIMATE VARIABILITY

Klaus M. Weickmann: Convection and Circulation Anomalies over the Oceanic Warm Pool during 1981-1982 623
Claire Perigaud: Instability Waves in the Tropical Pacific Observed with GEOSAT 637
Ryuichi Kawamura: Intraseasonal and Interannual Modes of Atmosphere-Ocean System Over the Tropical Western Pacific 649
David Gutzler, and **Tamara M. Wood**: Observed Structure of Convective Anomalies 659
Siri Jodha Khalsa: Remote Sensing of Atmospheric Thermodynamics in the Tropics 665
Bingrong Xu: Some Features of the Western Tropical Pacific: Surface Wind Field and its Influence on the Upper Ocean Thermal Structure 677
Bret A. Mullan: Influence of Southern Oscillation on New Zealand Weather 687
Kenneth S. Gage, Ben Basley, Warner Ecklund, D.A. Carter, and **John R. McAfee**: Wind Profiler Related Research in the Tropical Pacific 699
John Joseph Bates: Signature of a West Wind Convective Event in SSM/I Data 711
David S. Gutzler: Seasonal and Interannual Variability of the Madden-Julian Oscillation 723
Marie-Hélène Radenac: Fine Structure Variability in the Equatorial Western Pacific Ocean 735
George C. Reid, Kenneth S. Gage, and **John R. McAfee**: The Climatology of the Western Tropical Pacific: Analysis of the Radiosonde Data Base 741

Chung-Hsiung Sui, and Ka-Ming Lau: Multi-Scale Processes in the Equatorial Western Pacific 747
Stephen E. Zebiak: Diagnostic Studies of Pacific Surface Winds 757

MISCELLANEOUS

Rick J. Bailey, Helene E. Phillips, and Gary Meyers: Relevance to TOGA of Systematic XBT Errors 775
Jean Blanchot, Robert Le Borgne, Aubert Le Bouteiller, and Martine Rodier: ENSO Events and Consequences on Nutrient, Planktonic Biomass, and Production in the Western Tropical Pacific Ocean 785
Yves Dandonneau: Abnormal Bloom of Phytoplankton around 10°N in the Western Pacific during the 1982-83 ENSO 791
Cécile Dupouy: Sea Surface Chlorophyll Concentration in the South Western Tropical Pacific, as seen from NIMBUS Coastal Zone Color Scanner from 1979 to 1984 (New Caledonia and Vanuatu) 803
Michael Szabados, and Darren Wright: Field Evaluation of Real-Time XBT Systems 811
Pierre Rual: For a Better XBT Bathy-Message: Onboard Quality Control, plus a New Data Reduction Method 823